2017

Assessment Of A Function For Threonyl-Trna Synthetase In Angiogenesis In A Mouse Ovarian Cancer Model

Peibin Wo
University of Vermont

ASSESSMENT OF A FUNCTION FOR THREONYL-tRNA SYNTHETASE IN ANGIOGENESIS IN A MOUSE OVARIAN CANCER MODEL

A Thesis Presented

by

Peibin Wo

to

The Faculty of the Graduate College

of

The University of Vermont

In Partial Fulfillment of the Requirements
for the Degree of Master of Science
Specializing in Cellular, Molecular, and Biomedical Sciences

October, 2017

Defense Date: August 10, 2017
Thesis Examination Committee:

Karen M. Lounsbury, Ph.D., Advisor
Arti.Shukla, Ph.D., Chairperson
Alan K. Howe, Ph.D.
Cynthia J. Forehand, Ph.D., Dean of the Graduate College

ABSTRACT

Despite the high mortality rate of ovarian cancer, there are few selective biomarkers that detect its progression and none have become successful targets for therapy. A complex microenvironment that promotes angiogenesis, reduces immune responses and alters the integrity of the surrounding matrix is involved through the biology of ovarian cancer. Previous studies done by our lab and collaborators indicated that extracellular threonyl-tRNA synthetase (TARS) is a pro-angiogenic mediator of the ovarian tumor microenvironment, which is secreted in response to inflammatory signals, and actively promotes angiogenesis. In order to better understand the mechanisms underlying the angiogenic effects of TARS in ovarian cancer, it is essential to identify whether it directly affects ovarian tumor growth and invasion. Preliminary evidence indicated that TARS is secreted from ovarian cancer cells in response to TNF-α and TARS exhibits extracellular angiogenic activity. In previous studies, TARS was shown to significantly increase migration of HUVECs in a transwell assay to an extent that was similar to VEGF.

The purpose of this project was to establish a role for TARS in tumor progression and its potential as a diagnostic marker using an animal model of ovarian cancer. The hypothesis tested is that TARS plays a key role in the angiogenic and invasive potential of ovarian cancer, and TARS inhibition will reduce the angiogenic effect of tumor cells which is reflected by measurement of intratumor microvessel density (MVD). The study tested the effect of BC194-mediated TARS inhibition on the development of ovarian tumors in ID8 mouse model. We found a positive correlation between TARS expression and ovarian cancer progression, and TARS inhibition with BC194 reduce the progression of ovarian cancer. These data suggest that TARS has an important role in the tumor microenvironment and that TARS inhibition should be further investigated as a therapy for ovarian and other angiogenic cancers.

CITATIONS

Material from this dissertation has been published in the following form:

Mirando A.C., Abdi K, Wo P, and Lounsbury KM..(2017). Assessing the effects of threonyl-tRNA synthetase on angiogenesis-related responses. Methods, 113:132–138, 2017

DEDICATION

I would like to dedicate this work to my beloved parents and my son, whose support and sacrifices have laid the foundation for this accomplishment.

ACKNOWLEDGEMENTS

First and foremost I would like to express my sincerest gratitude to my advisor, Karen Lounsbury, whose guidance, patience, and curiosity have undoubtedly improved my skills and passion as a scientist. I am also very grateful for sharing my graduate experience with past and present members of the Lounsbury Lab and the Department of Pharmacology, especially Terry for her advice, assistance, and friendship have greatly enriched my studies in both fun and productive ways. I could not have asked for a better mentor and lab group.

TABLE OF CONTENTS

Page

LIST OF TABLES

LIST OF FIGURES

LIST OF ABBREVIATIONS

ARS – Aminoacyl-tRNA synthetase

BRCA– Breast cancer gene

CAM – Chorioallantoic membrane

CIAS – Automated cell counting technique

EGF – epidermal growth factor

FGF – Fibroblast growth factor

HIF-1α – Hypoxia inducible factor-1α

HOX – Homeotic genes

HUVEC – Human umbilical vein endothelial cell

IMA – Intratumor microvascular area

LARS – Leucyl-tRNA synthetase

MARS – Methionyl-tRNA synthetase

MVD – Microvascular density

NF-κB – Nuclear factor κ-light-chain-enhancer of activated B cells

OvCa – Ovarian cancer

PDGF – Platelet derived growth factor

SKOV – SKOV3 ovarian carcinoma cell line

TARS – Threonyl-tRNA synthetase

TNFα – Tumor necrosis factor α

WARS – Tryptophanyl-tRNA synthetase

VEGF – Vascular endothelial growth factor

VEGFR – Vascular endothelial growth factor receptor

YARS – tyrosyl-tRNA synthetase

CHAPTER 1: INTRODUCTION

1.1 Angiogenesis

1.1.1 Angiogenic process and regulators of angiogenesis

A number of sequential events are involved in the formation of a new blood vessel. For the ovary neovascularization, the cellular events are virtually identical no matter where the stimulus comes from. It could be either from periodic neovascularization of the normal ovarian follicle or from ovarian tumor cells (Brown, Blanchette et al. 2000). At a given time, endothelial cells exist in a near quiescent state with only 0.01% cells undergoing division prior to neovascularization. When a new vascular sprout forms, the turnover rate of endothelial cells increases up to 50-fold. In order to promote angiogenesis by unmasking pro-angiogenic molecules, remodeling of the extracellular matrix is required which is facilitated by secretion of matrix degrading enzymes (Baba, Mandai et al. 2004).

After the extracellular matrix is digested, motility-stimulating extracellular matrix fragments and growth factors are released to stimulate endothelial cells and create a framework for new vessels. Endothelial cell sprouts then proliferate and organize into tubular structures, form tight junctions and connect to the pre-existing vascular network. Angio-stimulatory molecules are secreted by non-endothelial cells and activated by surrounding stroma, which induce and maintain the angiogenic events. Physiological angiogenesis is basically a self-limited process and is regulated by endogenous angio-

inhibitory molecules. This balance of angiogenesis is disturbed during cancer progression.

Tumor cells are able to secrete molecular modulators which initiate the angiogenic process. The newly formed blood vessels provide oxygen and nutrients for further tumor growth to overcome the diffusion-limited maximal size of approximately 2 mm^3 of a tumor mass. This 'angiogenic switch', the acquisition of the angio-stimulatory phenotype results from a local imbalance between angio-stimulatory and angio-inhibitory molecules. Malignant cells and/or the stroma may increase the production of angio-stimulatory molecules (Glass, Quackenbush et al. 2015). Neovascularization increases blood flow, provides access for immune cells—which can also secrete angio-stimulatory molecules, and provides a means of egress for tumor cells, which finally become metastasis.

The balance of angio-stimulatory and angio-inhibitory molecules are kept by genetic regulation. A number of genes have been identified that regulate downstream molecules and pathways critical in angiogenesis, among which, P53 is a prominent one. P53 is a critical tumor-suppressor gene, been shown to participate in the control of gene transcription, DNA synthesis and repair, cell necrosis, tumor invasion and metastasis.

P53 is mutated in a majority of advanced stage ovarian cancers and is a potent prognosticator of poor clinical outcome (Glass, Quackenbush et al. 2015). Loss of wild-type p53 promotes angiogenesis by upregulating vascular endothelial growth factor (VEGF), which is a potent mitogen for endothelial cells. P53 mediates upregulation of

hypoxia inducible factor-1 (HIF-1α), which induces the VEGF increase. HIF-1 is an oxygen-regulated transcriptional factor, composed of two subunits HIF-1α and HIF-1β. HIF-1 is able to bind the 5' flanking regions of VEGF and activates VEGF transcription. Overall, loss of P53 enhances hypoxia-induced HIF-1α levels, induces HIF-1 dependent VEGF expression in tumor cells and promotes neovascularization of tumor xenografts (Glass, Quackenbush et al. 2015).

Angiogenesis is closely regulated by extracellular matrix (ECM) proteins through the integrin family of receptors. Integrins are divalent cation-dependent heterodimeric membrane glycoproteins comprised of non-covalently associated α and β subunits that promote cell attachment and migration on the surrounding extracellular matrix.

In vitro and *in vivo* data have implicated a number of endothelial cell integrins in the regulation of cell growth, survival and migration during angiogenesis. These integrins include the heterodimers α1β1, α2β1, α4β1, α5β1, α6β1, α6β4, α9β1, αvβ3 and αvβ5. Despite the conflicting theories and evidences of several integrins in angiogenesis, including αv integrins and α2β1 integrin, some major roles for key integrins have been revealed. The integrin αvβ3, a receptor for RGD-containing proteins such as vitronectin, fibronectin, fibrinogen and osteopontin (which are components of the ECM), was the first of the alpha v integrins to be characterized and shown to regulate angiogenesis (Brooks, Clark et al. 1994). This integrin is widely expressed on blood vessels in human tumor biopsies but not on vessels in normal human tissues. Its expression on endothelial cells is stimulated by angiogenic growth factors such as bFGF, TNFα, and IL-8 and it is

upregulated on endothelium in tumors, wounds and sites of inflammation (Brooks, Clark et al. 1994). Integrin αvβ3 antagonists induce endothelial cell apoptosis, increase the activity of the tumor suppressor p53 and increase levels of the cell cycle inhibitor p21 WAF1/CIP1 and decrease levels of the anti-apoptotic protein BAX. It was also shown that integrin αvβ3 promotes angiogenesis and endothelial cell survival and angiogenesis is cancelled by integrin suppression. Ligation of endothelial αvβ3 integrin has also been shown to activate MAP kinase, focal adhesion kinase (FAK) and Src, among other kinases, resulting in cell proliferation, differentiation and migration (Eliceiri, Klemke et al. 1998).

Fibronectin is key extracellular matrix protein that is deposited by endothelial cell during normal and tumor angiogenesis. Short fibronectin peptide loops containing the sequence RGD interact with integrin such as α5β1, αvβ5 and αvβ3 (Plow, Haas et al. 2000) Fibronectin is essential for developmental angiogenesis as deletion of all fibronectin isoform is early embryonic lethal, with yolk sac and other mesodermal tissue defects. The most recent fibronectin-binding integrin to be found to play a role in angiogenesis is integrin α9β1. It is a receptor for a number of ECM proteins and cell surface receptors including tenascin-C, thrombospondin, osteopontin, IIICS fibronectin, VCAM and other ligands (Marcinkiewicz, Taooka et al. 2000). Fibronectin and several of its receptors clearly play central roles in promoting angiogenesis during development and during tumor growth.

1.1.2 Angiogenesis and ovarian cancer

The complexity of genetic and/or environmental initiating events and lack of clarity regarding the cells or tissues of origin is a major hindrance to better understand how the ovarian cancer (OvCa) initiation and progression. A series of events are involved in metastasis, such as direct extension or exfoliation of cells into the peritoneal cavity, survival of matrix-detached cells in ascites, and subsequent adhesion to the mesothelium lining covering abdominal organs to establish secondary lesion containing host stromal and inflammatory components (Baba, Mandai et al. 2004). It's a remarkable challenge to develop experimental models to understand this unique mechanism of metastasis. Many approaches and knowledge used to study other solid tumors (lung, colon, and breast, for example) are not transferable to OvCa research given the fact that OvCa have distinct metastasis pattern and unique tumor microenvironment.

A correlation between clinical outcome and neovascularization of tumors, particularly in different OvCa subtypes, has been defined. Increased angiogenesis is a negative indicator of progression-free survival, overall survival, and predicts higher likelihood of metastasis in OvCa (He, Wang et al. 2015). Many factors such as tumor microvessel density and angiogenic cytokine expression as well as serum and urine levels of angio-stimulatory molecules have been used to study the role of angiogenesis as a prognosticator. Microvessel density is determined by counting the number of vessels which are stained immunohistochemically. Darai et al analyzed microvessel staining with CD31 (an endothelial marker, also known as PECAM) in 20 benign, 20 low malignant potential and 20 malignant ovarian tumors. Results found that microvessel counts in

ovarian cancers are higher than that of low malignant potential or benign tumors (Darai, Bringuier et al. 1998). A correlation between increased number of CD31-stained vessels and advanced stage and tumor grade was also observed. Orre et al found that microvessel counts are higher in mucinous than serous ovarian tumor subtypes, suggesting tumor vascularity may be associated with histological type (Orre, Lotfi-Miri et al. 1998). Hollingsworth et al. evaluated microvesssel density as a function of outcome in advanced stage ovarian carcinomas and found that increased microvessel density is associated with poor overall survival and shortened disease-free survival (Hollingsworth, Kohn et al. 1995). Angiogenesis has also been found to be a predictor of worse prognosis but not an independent variable in multivariate analysis. Abulafia et al used factor VIII staining to evaluate microvessel counts in primary and matched metastatic ovarian tumor samples. Microvessel counts in omental metastases, but not in primary ovarian tumors, correlated with pre-operative CA125 levels and patient survival (Abulafia, Triest et al. 1997). An association between angiogenesis and poor prognosis early stage ovarian cancers was also observed by Paley et al. in a study where they assessed VEGF expression through *in situ* hybridization of 68 stage I and II cancers (Paley, Goff et al. 2000).

1.1.3 Targeted therapy against angiogenesis in ovarian cancer (OvCa)

Angiogenesis not only plays a fundamental role in normal ovarian physiology but is also critically important in the pathogenesis of OvCa. Angiogenesis also promotes tumor growth and progression through ascites formation and metastatic spread. VEGF, fibroblast growth factor (FGF), and their respective receptors are among the well-

recognized promoters of angiogenesis. In addition, platelet-derived growth factor (PDGF), epidermal growth factor (EGF), angiopoietins, and hepatocyte growth factor are also known to involve in tumor angiogenesis (Paley 2002). OvCa cells express VEGF and VEGF receptor (VEGFR), and an association between VEGF expression and the development of malignant ascites and tumor progression has already established (Paley 2002).

Tumor growth is significantly decreased when tumor vascularization is reduced, and without adequate vascularization, tumor cells undergo necrosis or apoptosis. Most notably among those factors, VEGF has emerged as a dominant pathway although mechanisms underlying angiogenesis in tumors are multi-factorial and still quite unclear.

Among the various treatments for patients with platinum-resistant OvCa, anti-angiogenesis strategies are attractive. Bevacizumab (a monoclonal antibody to VEGF-α) was developed by Genentech, San Francisco, CA, USA and marketed as Avastin. In preclinical studies, bevacizumab used as maintenance therapy was shown to prolong survival by inhibiting or delaying disease recurrence in a murine OvCa model (Paley 2002). Bevacizumab is now the most prominent anti-angiogenic therapy approved by the Food and Drug Administration (FDA) for patients with platinum-resistant recurrent ovarian cancer as well as other angiogenic cancers including colon, renal and lung cancers. Combination of bevacizumab and cytotoxic chemotherapy has resulted in statistically improved cancer-free survival and overall response rate. Bevacizumab is also used as frontline therapy for ovarian cancer in many countries outside the United States.

1.1.4 Bevacizumab toxicity and adverse events

Although anti-VEGF therapy such as bevacizumab has been effective in OvCa, some severe complications such as gastrointestinal perforation, surgery and wound-healing complications, and hemorrhage have been reported. Bevacizumab was discontinued in 8.4%-21% of patients across all tumor types because of adverse reactions (Paley 2002). A better understanding of the mechanisms of bevacizumab adverse effects and resistance still need further investigations. The exact mechanism of resistance for anti-angiogenesis therapies is still not clear, but several pro-angiogenic pathways within the tumor, such as Angiopoietin 1, Delta-like ligand 4/Notch, and microRNAa), immune response, induction of hypoxia may be involved (Paley 2002).

1.2 Threonyl-tRNA synthetase

1.2.1 Introduction to threonyl-tRNA synthetase

Threonyl-tRNA synthetase (TARS) is a class II ARS which catalyzes the attachment of threonine to its corresponding tRNA for use in translation. TARS has a molecular weight of 83kDa (human, monomer; 76 kDa *E.coli*). However, like other class II ARSs, the protein is typically found as a homodimer. There are four core domains conserved from prokaryotes to eukaryotes in the structure of TARS. Although TARS has been implied in angiogenesis and tumor cell growth, its role in extracellular signaling had not been studied previously before the Lounsbury and Francklyn labs' work (Williams, Mirando et al. 2013).

1.2.2 Non-canonical functions of threonyl-tRNA synthetase

The canonical function of aminoacyl-tRNA synthetases (ARSs) is to attach amino acids to their cognate tRNAs a part of the protein synthesis machinery. Distinct non-canonical functions of many ARSs in eukaryotes have been found, such as inflammatory response regulation, transcriptional regulation, gene silencing, etc. These secondary functions may explain the links between ARSs and diverse human diseases. For example, correlations have been found between mutations in ARS and several nervous system-related disorders such as Charcot-Marie-Tooth disease, leukoencephalopathy, infantile encephalopathy, and a Type III Usher-like syndrome (Jordanova, Irobi et al. 2006). The distinct mechanisms that connect ARS activity with the pathogenesis of these diseases and the other non-canonical activities are still not clear, indicating that ARSs are dynamic signaling molecules functioning beyond established roles. Some extracellular signaling functions of several class I ARSs have been shown in previous studies, which are stimulated by inflammatory response, and they display different roles in angiogenesis. Tyrosyl-rRNA synthetase (YARS) and tryptophanyl-tRNA synthetase (WARS) are secreted in response to the cytokines TNF-α and interferon, respectively. While a secreted cleavage fragment of YARS is found to be angiogenic, a splice variant of WARS is secreted and inhibits angiogenesis (Wakasugi and Schimmel 1999).

Threnonyl-tRNA synthetase (TARS) has not been previously associated with extracellular signaling, although there are findings implying that it may be involved in angiogenesis and tumor cell growth. The macrolide antibiotic borrelidin, a potent non-competitive inhibitor of TARS, inhibits endothelial cell tube formation and reduces

metastasis in a mouse model of melanoma (Habibi, Ogloff et al. 2012). Among several derivatives of the original drug borrelidin, BC194 is less cytotoxic but retains the anti-angiogenic properties of borrelidin, making it a good candidate to study the mechanism of TARS regulating angiogenesis (Moss, Carletti et al. 2006).

In a previous study done by the Lounsbury lab, TARS was found to be actively secreted and to exert angiogenic activity, including stimulation of endothelial cell migration. Based on the data from the study, a model of the mechanism of how TARS functions in angiogenesis was presented (**Fig. 1**) (Williams, Mirando et al. 2013). Although the form of TARS that is secreted and its putative receptors still remain unclear, that study implied TARS has a novel extracellular function, confirming TARS as the anti-angiogenic target of the borrelidin derivative BC194, and indicating secreted TARS probably has a role in angiogenesis and inflammation in cancer and autoimmune

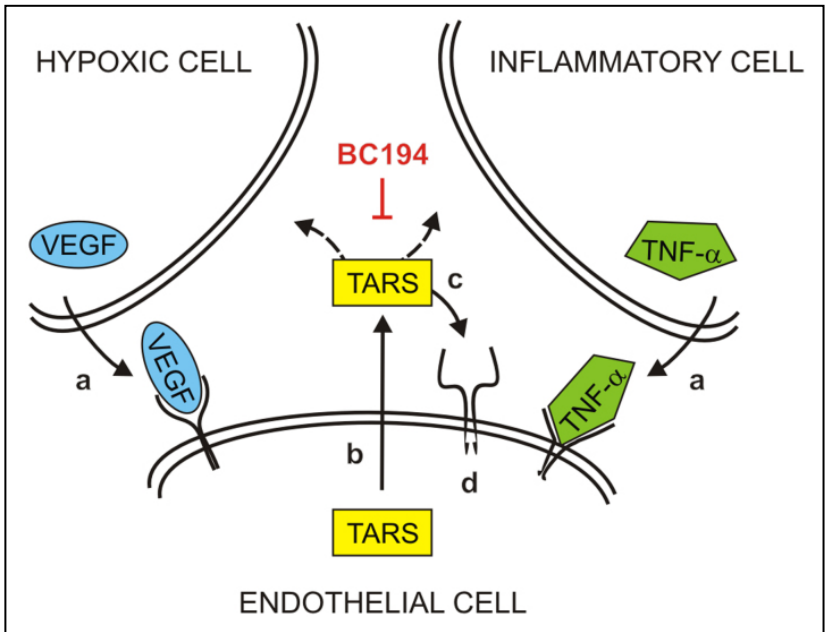

Figure. 1 Proposed model for TARS angiogenic activity. Modified from Williams et al. (11).

disease (Williams, Mirando et al. 2013).

1.2.3 TARS and ovarian cancer

Ovarian cancer is a highly angiogenic malignancy, and correlation between ovarian cancer progression and expression of angiogenic signaling molecules has already been established in many studies, two notables among these molecules are hypoxia-inducible factor (HIF-1α) and vascular endothelial growth factor (VEGF). In a previous study done by Lounsbury lab, a relationship between TARS and human ovarian cancer was explored. It was found that levels of TARS in patient tumor and inflammatory cells correlate with angiogenesis and stage of disease (Wong, Wellman et al. 2003).

In a study done by the Lounsbury lab, TARS expression in human ovarian cancer specimens was measured. Experiments were design to detect only overexpressed TARS. A significant positive correlation between increasing disease stage and TARS staining intensity was revealed. Overexpressed TARS also co-localized with VEGF and was in proximity to areas of neovascularization indicated by the endothelial marker PECAM (CD31) (Wellman, Eckenstein et al. 2014). These data suggest there is a novel relationship between TARS expression and ovarian cancer, and indicates an association between TARS and its angiogenic roles in the ovarian cancer microenvironment. In the same study, it was also found that TARS was overexpressed in infiltrating leukocytes within ovarian tumors, TARS was secreted from ovarian cancer cells in response to cell stress, serum levels of TARS correlated with tumor levels of TARS, overexpression of TARS correlated with increased survival in late-stage disease. All of these evidences

supported a connection between TARS and both angiogenesis and stage of ovarian cancer.

1.3 Ovarian cancer

1.3.1 Epidemiology and risk factors

Ovarian cancer is the sixth most common cancer in women (Vaughan, Coward et al. 2011). Among many subtypes, epithelial ovarian cancer is the most common, which results from malignant transformation of the ovarian surface epithelium. The disease is frequently presented in advanced stage and has a poor prognosis with present therapies. Incidence of epithelial ovarian cancer ranks high in Europe, the USA, and Israel, and relatively low in Japan and developing countries. The median age of patients is 60 years, and the average lifetime risk for women in developed countries is about one in 70. Family history of ovarian or breast cancer is found the most important risk factor, although a genetic predisposition (most notably breast cancer genes BRCA1/BRCA2 mutations) is present in only 10-15% of patients. For a woman with a BRCA1 mutation, the risk of epithelial ovarian cancer is 39-46%, and with a BRCA2 mutation, 12-20% (Christie and Oehler 2006). Lack of childbirth, early menarche, late menopause, and increasing age are also risk factors, whereas oral contraceptive use, pregnancy, tubal ligation, lactation could lower the risk.

1.3.2 Pathology of ovarian cancer

Epithelial ovarian cancers could either be serous (most common), mucinous, or endometrioid and less commonly clear cell, transitional, etc. Histologically, epithelial ovarian cancers are classified as grade 1, 2, 3 (Kaku, Watanabe et al. 2012). Embryonic origin of epithelial ovarian cancers come from the ovarian surface epithelium and the peritoneal and fallopian tube epithelia, although some ovarian cancers might originate from the distal tubes. Mucinous and endometrioid carcinomas usually have favorable prognoses, serous carcinomas less so, and undifferentiated carcinoma is the most aggressive subtype. Tumor grade is always a consistent prognosticator (Kaku, Watanabe et al. 2012).

1.3.3 Causes and pathogenesis

The majority (approximately 90%) of ovarian tumors arise from the ovarian surface epithelium, which completely covers the surface of the ovary and is continuous with the abdominal mesothelium. Gonadotropin receptors are expressed in epithelial cells, which interact with the ovarian stroma in the secretion of growth factors, cytokines, and steroids. The surface epithelial layer is disrupted after ovulation, and epithelial cells frequently grow into the stroma to form clefts or inclusion cysts. It was demonstrated in many studies that ovarian cancer originates from these clefts and inclusion cysts due to the interaction with the stromal environment full of hormones and growth factors. A number of subtypes of epithelial ovarian cancer have been identified histologically, with

approximately 80% of the classified as papillary serous epithelial (Kaku, Watanabe et al. 2012).

For the different subtypes of epithelial ovarian cancer, despite the possession of unique molecular mutation and transcriptional abnormality, their morphology usually resembles the specialized epithelia of the reproductive tract that originate from the Mullerian ducts. Research suggests that epithelial ovarian cancer might all arise from one precursor cell of surface epithelium where homeotic genes (HOX genes) regulate embryonic pathways of differentiation. HOX genes are not usually expressed in ovarian surface epithelium. However, introduction of expression of HOXA9, HOXA10, and HOXA11 to ovarian surface epithelium in tumorigenic mice is able to lead these cells to differentiate along different mullerian lineages, giving rise to tumors with characteristics of serous, endometrioid, and mucinous ovarian tumors, respectively (Kelly, Michael et al. 2011). It was also found that HOXA7 controls the extent of differentiation and grade of ovarian tumors (Christie and Oehler 2006). Since HOX gene expression is regulated by sex steroids throughout the menstrual cycle, over-exposure of ovarian surface epithelium cells to these hormones in adult women might lead to abnormal HOX activation, leading to proliferation and genomic instability.

Genomic mutations have a critical role in the pathogenesis of many forms of epithelial ovarian cancer. It has been reported that high-prevalence somatic (non-germline) mutations (>5%) only exist in a small number of genes in epithelial ovarian cancer(Christie and Oehler 2006). These mutations affect the pathogenesis in a similar

manner like HOX. These genes includeTP53, CTNNB1, and PTEN (all inactivated), and KRAS, Pik3CA, and AKT1 (all activated).

1.3.4 Staging of ovarian cancer

In summary, there are four stages of the disease correspond to (I) ovarian, (II) pelvic, (III) peritoneal or coelomic, and (IV) metastasizing disease. Staging of epithelial ovarian cancers is shown in **Table 1 (Mutch and Prat 2014)**. From the primary tumor, propagation can occur throughout the abdominopelvic peritoneal compartment and to retroperitoneal pelvic, periaortic, suprarenal, mesenteric, and mesocolic lymph nodes. The most common extra-abdominal site of disease is the pleural space. Less frequently, distant metastases occur in the parenchyma of the liver, lungs, and other organs (Mutch and Prat 2014).

Table 1: Ovarian cancer staging by International Federation of gynecology and obstetrics criteria

Stage I: tumor restricted to ovary
IA : limited to one ovary; capsules intact, no tumor on ovarian surface; no malignant cells in ascites or peritoneal washings
IB: limited to both ovaries; capsules intact, no tumor on ovarian surface; no malignant cells in ascites or peritoneal washings
IC: tumor limited to one or both ovaries with capsule rupture or tumor on ovarian surface; malignant cells in ascites or peritoneal washings
Stage II: tumor involves one or both ovaries with pelvic extensions
IIA: extension or implants on uterus or tubes, or both ;no malignant cells in ascites or

peritoneal washings
IIB: extension to other pelvic tissues; no malignant cells in ascites or peritoneal washings
IIC: pelvic extension with malignant cells in ascites or peritoneal wshings
Stage III: tumor involves one or both ovaries with peritoneal metastasis outside the pelvis or retroperitoneal or inguinal node metastasis
IIIA: microscopic peritoneal metastasis beyond pelvis
IIIB: macroscopic peritoneal metastasis beyond pelvis 2 cm or less in greatest dimension
IIIC: peritoneal metastasis beyond pelvis more than 2 cm in greatest dimension or regional lymph node metastasis, or both.
Stage IV: distant metastasis(excludes peritoneal metastasis) to liver parenchyma or other visceral organs or a malignant pleural effusion

1.3. Markers for ovarian cancer

Identification of tumor markers and development of assays to measure them is an important goal in oncology. It is also important in differential diagnosis in order to establish appropriate management. It is difficult to distinguish diffuse peritoneal malignant mesothelioma from ovarian cancer, but differential diagnosis can be achieved by immune profile of the tumors with a systematic approach of both positive and negative mesothelioma markers (Hassan, Remaley et al. 2006).

Immunohistochemistry is used to achieve the definite diagnosis. Podoplanin, calretini, CK5/6, WT1, thrombomodulin, mesothelin, and D2-40 antibodies are used as positive markers of mesothelioma that are commonly expressed in mesotheliomas, but not in carcinomas, while Ber-EP4, MOC-31, TAG72, CA19-9, CD15(Leu-M1), monoclonal CEA and BG-antibodies are negative markers for mesothelioma that are

commonly expressed in adenocarcinomas(Taskin, Gumus et al. 2012). Mesothelin is highly sensitive for malignant mesothelioma, but its specificity is relatively low because some other tumors including ovarian cancer also exhibit mesothelin positivity. Nevertheless diffuse and strong membranous mesothelin expression serves as a strong indicator of particularly epitheliod mesothelioma rather than an ovarian carcinoma (Ordonez 2007).

Another distinguishing marker for ovarian cancer is estrogen receptor (ER) positivity. ER expression in malignant mesothelioma is a very rare phenomenon, and its positivity most probably indicates a serous carcinoma rather than a mesothelioma. Malignant mesotheliomas can be referred to gynecologic oncology clinics with primary ovarian masses or peritoneal carcinomatosis. This rate was calculated as 0.1% in one study (Taskin, Gumus et al. 2012). Clinical distinction of malignant mesothelioma from ovarian cancer or peritoneal adenocarcinoma is considered very difficult, but can be achieved by immune profile of the tumors.

1.4. Modeling of ovarian cancer

1.4.1 Cell lines and xenografts

Auersperg et al. first isolated human ovarian surface epithelial (OSE) cells in 1984, which allowed the development of initial ovarian cancer models to evaluate the efficacy of the chemotherapy (Liu, Yang et al. 2004). These models typically involved the injection of human OvCa cells subcutaneously, intraperitoneally or orthotopically into immune deficient mice. A variety of responses of different levels occur, such as ascites

formation, primary tumor spread and tumor progression. All of these are helpful for the researcher to better understand the underlying mechanism of the disease. However, the limitations of this approach are evident with some drawbacks such as lack of the initial tumor-ovary interaction and the absence of an intact immune system in the host mice, while immune system has been implicated as a very important mediator of cancer progression and metastasis by many studies.

Although a number of ovarian cancer cell lines and primary tissues are currently available to mimic the molecular diversity, cellular heterogeneity, and histology seen in patient tumors, no uniform collection exists. Several human ovarian cancer cell lines can be used for xenograft studies in mice. Examples of the human cell lines which are suitable for development as murine xenografts are OVCAR-3 and SKOV3 (Peterson, Reed et al. 1992). OVCAR-3 has been successfully grown in mice and develops as an intraperitoneal xenograft that retains many characteristics corresponding to its human tumor counterpart, similar to a serous ovarian cancer. The ovarian cancer cell line SKOV3 was collected from a patient in relapse after cisplatin and chlorambucil treatment and represents well differentiated serous adenocarcinoma cell lines, which is able to form xenograft tumors with a very similar histology to a human serous cancer. Several sublines of SKOV3 cells were made by passaging the cells in nude mice. In nude mice, the SKOV3 cells grow as disseminated disease, numerous (100-200) small nodules could be found on the surface of the peritoneum bowel mesentery, and diaphragm. Mouse omentum could also be transformed into a large tumor, mimicking human advanced stage serous-papillary OvCa.

The development of mouse OvCa cell lines for use in syngeneic mouse models has the advantage of use in immunocompetent mouse models. For these models, mouse ovarian epithelial cells are collected from the mouse bursa and are passaged in culture until phenotypic changes occur. For example, cell contact inhibition could be lost, leading to changes in cell morphology. Neoplastic progression in the cell culture dish often includes the loss of tumor-suppressor proteins E-cadherin and connexin-43 (Roby, Taylor et al. 2000).

Ascites and metastatic tumors form 90 days after transformed OvCa cells are injected intraperitoneally into C57BL/6 mice, while solid tumor forms confining to the injection area if cells are injected subcutaneously. The significant disadvantage of the intraperitoneal model is that early events in metastasis cannot be fully appreciated, because the initial steps of tumor formation rely on the artificial dispersion of single cell suspensions of cancer cells in the peritoneal cavity, rather than progression of metastasis from an intact primary tumor tissue (Roby, Taylor et al. 2000).

The method of orthotopic ovarian xenografts is developed to better mimic the process of dissemination from the primary ovarian tumor relative to the intraperitoneal xenografts discussed above, and may be better for studying metastasis. However, significant anatomic differences exist between rodents and humans. The ovary of the rodents has a closed bursa enclosing it, while the ovary of the humans is exposed to the peritoneal cavity.

Several methods have been developed for orthotopic mouse models: injection under the ovarian bursa, intraperitoneal injection of minced human tumors, implantation

of human or murine tumor fragments adjacent to the ovary. Critical steps involved in ovarian cancer metastasis are invasion though the ovarian bursa, followed by peritoneal cavity spread and colonization and invasion of organs in the peritoneal cavity. When late passage cells from the mouse ovarian epithelial cancer cell line MOSEC were injected into athymic and syngeneic mice, tumor implants grew throughout the abdominal cavity, and produced hemorrhagic ascitic fluid. A highly malignant neoplasm resulted with both carcinomatuous and sarcomatous components. The ability and pattern that MOSEC form extensive tumors within the peritoneal cavity is very similar to stage III and IV ovarian cancer found in women (Roby, Taylor et al. 2000). Since in the syngeneic mice model, the immune systems are intact in mice, the ability of MOSEC to form extensive tumors within peritoneal cavity despite the immune response they dealt with, makes this model uniquely valuable for investigations of molecular and immune interactions in ovarian cancer development.

1.4.2 ID8 mouse model

In this project, the role of TARS in ovarian cancer were studied in a mouse model of ovarian cancer first described by Roby et al. (Roby, Taylor et al. 2000). This model was developed by propagating normal mouse ovarian surface epithelial cells in culture for multiple passages until they developed a transformed phenotype. Intraperitoneal or subcutaneous transplantation of the cells into standard C57BL/6 mice resulted in tumors and peritoneal ascites. As opposed to a xenograft model using human tumor lines in immunocompromised mice, the syngeneic nature of the ovarian model

allows the tumor-stromal interactions characteristic of genuine cancers to be more accurately reproduced.

1.4.3 ID8 cell gene status

The TP53 tumor suppressor gene has long been established as a critical regulator of cell proliferation and as a frequent target for mutation in cancer (Greenblatt, Bennett et al. 1994). The TCGA project identified *TP53* mutations in 96% of ovarian cancers (Cancer Genome Atlas Research 2011). Whole-exome sequencing has been performed to assess the genomic landscape of the ID8 cell model to identify the functional mutations in genes characteristic of HGSC including Trp53 (the mouse p53 gene), however, no Trp53 mutations were detected (Walton, Blagih et al. 2016). Some mutations typically seen in clear cell (*Pik3ca*), low-grade serous (*Braf*), endometrioid (*Ctnnb1*), and mucinous (*Kras*) carcinomas were also notably not observed (Walton, Blagih et al. 2016).

Given the centrality of TP53 mutations in HGSC, p53 function was also assessed in ID8 cells, and a significant increase of p53 function was observed (Walton, Blagih et al. 2016). Following treatment with cisplatin and MDM2 inhibitor Nutlin-3, a marked increase in CDKN1A (p21) transcription was also detected, indicating that p53 remains transcriptionally active. For intraperitoneal ID8 tumors, Sanger sequencing didn't find Trp53 mutation in any tumor, including common hotspot mutations sites, and a wild –type pattern of p53 expression was confirmed with immunohistochemistry (Walton, Blagih et al. 2016). IHC examination of typical HGSC markers indicated that tumors were strongly and diffusely positive for WT1, but negative for PAX8. For Brca2, no functional abnormalities was identified in whole-exome sequencing. It was considered

that parental ID8 cells were able to form Rad51 foci in response to DNA DSB damage Together, these data suggest that parent ID8 is poorly representative of human HGSC (Walton, Blagih et al. 2016).

Roberts et al. compared the alterations of the actin cytoskeleton as well as expression of cellular adhesion proteins versus the number of passages to study the progression of ovarian carcinogenesis, showing that transformation from a premalignant to a highly malignant phenotype with downregulation of E-cadherin and connexin-43 (Roberts, Mottillo et al. 2005).

In a study done by Greenaway et al.(Greenaway, Moorehead et al. 2008), ID8 cells were injected into the ovarian bursal cavity of C57bL6 mice. The ID8 formed direct contact with the ovarian stroma, resulting in primary tumor formation, secondary peritoneal tumors, and extensive ascites fluid. The histological and gross pathological features resembled serous carcinoma. Increased expression of proliferative and survival markers, including phosphorylated Akt, proliferating cell nuclear antigen, and Bcl-2, were increased. VEGF levels were also increased in the serum and ascetic fluid.

Based on these findings, it seems that ID8, a widely used murine model of ovarian carcinoma, is a poor representative of HGSC, with a conspicuous absence of mutations in genes associated with human disease, and evidence of functional p53 activity. It remains, however, a useful model due to its origin and ability to consistently form tumors that closely parallel the patterns seen in HGSC.

Genetically engineered mouse models of HGSC have been difficult to generate. Recently, two HGSC models were described: the Drapkin lab utilized the Pax8 promoter

to drive Cre-mediated recombination of Trp53 and Pten with Brca 1 or Brca2 in mouse fallopian tube secretory epithelium (Perets, Wyant et al. 2013). By morphology and IHC, the tumors resembled human HGSC, but no ascites was observed, and all *Pten*$^{-/-}$ mice developed endometrial lesions. In addition, no transplantable cell lines have been described from these mice. A second fallopian tube model has been described, with SV40 large T antigen under the control of the *OVGP-1* promoter. Again, STIC-like lesions with p53 signatures were described, as well as invasive tumors within the ovary. However, no peritoneal dissemination or ascites was seen, and, again, no lines that can be readily transplanted into nontransgenic mice have been described (Sherman-Baust, Kuhn et al. 2014). Both of these models are undoubtedly of great importance. However, it was believed that a transplantable model, based on a single genetic background (C57BL/6), which recapitulates disseminated peritoneal disease with ascites and in which multiple genotypes can potentially be rapidly investigated in parallel, is an important adjunct to transgenic models.

1.5 Quantification of Angiogenesis

1.5.1 Microvessel density (MVD)

Many angiogenesis assays have been developed to assess the new blood vessel growth, including chick chorioallantoic membrane (CAM) assay, the corneal micropocket assay, dorsal skin fold chamber, and matrigel assay. Notably, tumor angiogenesis can be directly studied in solid tumor tissue specimens. The focus of this project was to determine the role of TARS activity in the vascularization of tumors in

developing ovarian tumors. For this purpose, we used the most widely used method of quantifying new blood vessel growth: the determination of intratumoral microvessel density (MVD) (Wild, Ramakrishnan et al. 2000).

The degree of angiogenesis of a tumor, as assessed by MVD, is a powerful candidate for prognosis and a predictive tool. The College of American Pathologists has investigated the prognostic and predictive factors in breast cancer and has ranked quantification of tumor angiogenesis by counting microvessels in immunostained tissue sections as category III evidence (Vermeulen, Gasparini et al. 2002). In a multivariate analysis, MVD was found to be the most accurate prognostic indicator in breast carcinoma for disease-free survival (He, Wang et al. 2015); better than size, grade, or estrogen receptor status.

1.5.2 MVD Test Methods

Intra-tumor microvessels can be identified by immunostaining of endothelial cells. There are two kinds of human endothelial cell specific antibodies: the pan-endothelial cells markers and antibodies that bind selectively to activated or proliferating endothelium. The pan-endothelial cell markers stain small and large vessels with equal intensity, and in both frozen and paraffin embedded samples with equal reactivity (Hasan, Byers et al. 2002).

The most commonly used antibodies include those against factor VIII related antigen, CD31/PECAM-1, and CD34. Factor VIII related antigen forms part of the von Willebrand factor (vWF) complex and plays a role in the coagulation process (Charpin,

Garcia et al. 1997). The platelet-endothelial cell adhesion molecule CD31/PECAM-1, is a transmembrane glycoprotein involved in cell adhesion, and CD34 is a surface glycoprotein of unknown function (Charpin, Garcia et al. 1997).

Previous investigations on MVD in prostate cancer have demonstrated remarkable differences between vWF-MVD and CD34-MVD as well as CD31-MVD and CD34-MVD(Offersen, Borre et al. 2002). A quite heterogeneous staining pattern of endothelial cells for the three markers was observed in prostate cancer tissue: a significantly increased MVD was only reflected when the two endothelial markers, CD31 and CD34, were used whereas vWF showed a significantly decreased number of microvessels in prostate cancer compared to benign BPH tissue. In prostate cancer specimens, benign tissue is displaced by invasive tissue, resulting in a decreased number of pre-existing mature microvesssels, which are visualized by vWF. Therefore, vWF is suitable marker for endothelial cells in benign tissue, but would seem to be an inferior marker for assessing newly developed microvessels in prostate cancer(Offersen, Borre et al. 2002).

The investigation on astrocytoma and oligodendroglioma are in accordance with our findings in prostate cancer: CD34 showed the highest sensitivity for vascular endothelial cells compared to CD31 and vWF. Accordingly, the specificity of CD34 for endothelial cells is higher in malignant tumors than in more differentiated tumor entities.

The relative abilities of these antibodies to highlight the vasculature has aslo been examined in EOC. Detection of blood vesssels in tissue sections has recently been modified so that it is now possible to discriminate between newly formed immature

vessels and those that are more established and mature. Antibodies to α smooth muscle actin (α-SMA) appear to stain mature vessels because they attract a “coat” of periendothelial support cells—that is, pericytes and smooth muscle (α-SMA positive) cells. Antiangiogenic therapeutic procedures, such as the blockade of tumor cell VEGF production, result not only in a drop in the vessel count, but also a change in the ratio of immature/mature vessels because of the relative vulnerability of the immature vessels to this, and most other, forms of antiangiogenic treatment(Bamberger and Perrett 2002).

The problem of antigen specificity is highlighted by the detection of CD34 antigen on lymphatic vessels, perivascular stromal cells as well as other stromal elements while this is compounded by the absence of FVIII-RA on part of the capillary endothelium in tumor tissue. The disadvantages associated with staining for CD31 antigen include co-staining of inflammatory cells, but these can be distinguished from endothelial cells on the basis of morphological differences, and frequent antigen loss due to fixatives that contain acetic acid. Microwave antigen retrieval effectively abolishes this problem but in prospective studies a careful selection of the most suitable tissue fixation procedure should still be performed.

Despite the fact that MVD is identified as an independent prognostic factor in solid tumors, several studies have questioned the finding. Besides the particular tumor biological factors that may obscure the relationship, other issues such as staining methodology have also been implicated. Lack of standardized immunohistochemical techniques because of the wide range of antibodies, antigen retrieval methods, designation of high and low vessel count groups (cut-off points), patient groups, vessel

quantification interpretation could all contribute to the discrepancy. The correct identification of the vascular hot spot within the tumor and observer experience are two of the most important factors. In one study that compared the effects of different methodologies on evaluation of tumor vascularity, specimens of breast, lung and oral carcinoma and normal breast tissue were investigated. A variety of factors such as pretreatment of sections (enzymatic digestion, heating), endothelial markers (von Willebrand factor or CD31 antibodies), method of quantification (highest microvascular density, average microvascular density and microvascular volume) and inter-observer variations were all found to alter the estimated vascularity (28). Notably, the pretreatment of sections before staining was found to be the variable that most significantly altered the calculated vascularity of tumors.

An international consensus on the methodology and criteria for evaluation of MVD was put forward to overcome some of the problems of discrepancy (Vermeulen, Gasparini et al. 2002). In this consensus, a standard method for MVD assessment was proposed to improve reproducibility and inter-observer compatibility with regard to the selection of representative tissue samples, tissue processing and immunostaining, selection of areas for microvessel calculation and vessel counting method within these areas. Given the subjective nature of vascular hot spot selection and individual microvessels identification, a training program for the inexperienced pathologist is also recommended.

1.5.5 Microvessel density and metastasis

Several studies have examined the connection between MVD and tumor progression and metastasis (30). A correlation between MVD, intravascular tumor cells and the pulmonary metastasis was reported in an animal tumor model more than 20 years ago, but was not confirmed concerning its clinical implications. It was shown in one research study that patients with a high vascular density had more frequent tumor cell shedding than patients with a low MVD. In another investigation concerning cutaneous melanoma, it was found that angiogenesis intensity in a human tumor is a good predictor for the probability of metastasis (Massi, Franchi et al. 2002).

The significance of tumor vascularity in clear cell renal cell carcinoma has been controversial, partly because the manual quantification of MVD within a small area of tumor was limited. In the study, MVD and vascular endothelial growth factor were assessed in both areas of tumor and normal kidney medulla within scanned images using imaging software. CD34 staining vessels were counted and intensity of VEGF staining measured. To improve the accuracies of manual quantification, a computerized image analysis was employed, which allowed assessment of large areas of tumor and surrounding normal tissue. The latter was used as an internal reference for normalization. Original values from tumor areas and adjusted values as tumor/normal ratios were obtained. It was reported there was no association between unadjusted MVD and clinical outcome. However, higher adjusted MVD was associated with shorter disease-free survival. The validity of manual counting has been questioned since its introduction, and computerized image analysis still needs improvement to satisfy the potential bias in calculating tumor MVD.

1.6. Summary and hypothesis

Ovarian cancer is a vicious malignancy with extraordinarily high mortality rate. There are few selective biomarkers that detect its progression and none have become successful targets for therapy. A complex microenvironment that promotes angiogenesis of the disease is deeply involved in the ovarian cancer progression and metastasis.

TARS is a member of the ARS enzyme family with the canonical function to catalyze ATP-dependent formation of specific amnio-acyl tRNAs. A variety of non-canonical functions of several ARSs were found, such as inflammatory regulation, cell migration modulation and angiogenesis.

Angiogenesis has been established a critical component of the tumor microenvironment, and anti-angiogenic therapies using the VEGF inhibitor bevacizumab for ovarian cancer have shown effectiveness. Although these therapies have shown a variety of extent of efficacies in patients with ovarian cancer, the treatment complications and lack of success in some patients lead to the exploration of new ovarian-specific angiogenic targets.

In previous studies, several aspects of the non-canonical functions of TARS have been reported. TARS has been associated with autoimmune disorders including polymyositis and dermatomyositis through its identification as the target for the myositis autoantibody PL-7 (Howard, Dong et al. 2002). TARS was also detected in a genome-wide RNAi screen for genes associated with protection from hypoxia. The studies done by the Lounsbury lab demonstrated that TARS was secreted from ovarian cancer cells in

response to TNF-α, exhibited extracellular angiogenic activity, and was able to induce endothelial cell migration. The studies also indicated that TARS was overexpressed in ovarian cancer, TARS was found to be expressed in colocalization with VEGF and its expression was positively correlated with ovarian cancer stage. In addition, analysis of TARS levels in patient serum samples showed a positive correlation with TARS tumor levels.

All of these evidence and observations suggest several important questions to be resolved: is TARS protein expression characteristic of tumor development, and if so, at what stage of cancer development? Is such expression coincident with expression of angiogenic markers and/or vascularization? With our patient data as precedent, we examined these questions in the ID8 mouse model of ovarian cancer that has been well characterized and has the flexibility of altering TARS expression to determine its specific role in the growth and vascularization of tumors.

CHAPTER 2: METHODS

2.1 Cell culture and reagents

The ID8-C3 cell line we used to generate ovarian tumors was originally generated by self-transformation of normal mouse ovarian epithelial cells and were generously supplied by Brent Berwin (Dartmouth College) (Roby, Taylor et al. 2000). ID8-C3 cell were cultured and propagated by serial passage in RPMI media supplemented with 10% fetal bovine serum and 0.1% gentamycin sulfate. After being injected into the mice intraperitoneally, these cells form tumors which mimic stage IV human ovarian cancer (Erickson, Conner et al. 2013). BC194 was obtained from Biotica (now Isomerase Therapeutics Ltd, Cambridge, UK).

2.2 Mouse modeling by injecting ID8-C3 ovarian cancer cells

C57BL/6 mice were used for ovarian cancer modeling and assessment of tumor formation. All the experiments performed in animals were in compliance with IACUC protocols (IACUC #13-044). Mice were housed 3 per cage in the standard mice plexiglass cages and maintained on a 12 h light: 12 h dark cycle (lights on at 7.00 a.m) in a temperature-controlled room (22±2°C) with food and water ad libitum at all times.

The injection protocol followed the previous research (Roby, Taylor et al. 2000). For injections, ID8-C3 cell were grown in culture, collected by trypsinization and centrifugation, and then resuspended in PBS. 3×10^6 cells were injected intraperitoneally into normal six-week-old female C57BL/6 mice (Mirando, Abdi et al. 2016). Intraperitoneal tumor formation was monitored by the accumulation of ascites fluid

(Roby, Taylor et al. 2000). For specific experiments, three weeks after the cell injection, mice were administered vehicle (DMSO) or the TARS inhibitor BC194 (2 mg/kg intraperitoneally 3 times per week for 3 weeks). After injections, the mice were evaluated 3 times every week for the development of ascites by detecting abdominal swelling. The mice were euthanized 6-8 weeks after the initial injection. At the time of death, ascites fluid was collected from the peritoneal cavity using 10 cc syringe fitted with a 22 g needle. Blood was also collected in heparin solution, and was serum obtained by centrifugation. The abdominal cavity was opened with a single midline incision, tumors in the abdominal cavity were photographed and tumor locations and sizes were noted for staging. As described in (Roby, Taylor et al. 2000), amount of tumor on tissues and organs was scored on a 0, +, ++, +++ scale: **see Table 2**. Tumors and surrounding tissues were collected from multiple sites, fixed in 4% paraformaldehyde and embedded in

Table 2: Description of Tumor scoring

Tumor Score	Description of tumors
0	No tumor evident by gross examination
+	Tumors grossly evident on one organ or tissue
++	Moderate tumor formation on more than one organ or tissue
+++	Extensive tumor formation on several organs or tissues

paraffin for future analysis by immunofluorescence and to quantify MVD.

2.3 Immunofluorescence analysis

Serial sections (5μm) from paraffin-embedded specimens were cut and transferred to positive ion-charged slides. The slides were then deparaffinized and rehydrated by use of xylene, 100% ethanol, 95% ethanol, 70% ethanol, 50% ethanol, followed by a thorough wash with deionized water. Slides were treated with antigen retrieval buffer Dako S1699 for 20 minutes at 95-98°C. After at least 20 minutes cooling, slides were blocked with 3% BSA/0.2% TX-100/PBS for one hour at room temperature, followed by incubation with primary antibodies as described in **Table 3.** Slides were

Table 3: Primary antibodies used for Immunofluorescence

Primary antibody	**Product #**	**species**	**dilution**
anti-ThrRS	GTX116359	Rabbit	1:400
anti-SMactin	Sigma A2547	Mouse	1:200
anti-CD3	Biocare CP215A	Rabbit	1:100
anti-PECAM-1	SC-1506	Goat	1:100

Table 4: Secondary antibodies used for Immunofluorescence

Secondary antibody	**dilution**
Alexa 488 donkey anti-ms IgG	1:500
Alexa 594 donkey anti-rab IgG	1:500
Alexa 488 donkey anti-goat IgG	1:500

incubated in a humidified box at 4 °C for 16–24 h and then washed several times in a Coplin jar with PBS. All antibodies were titrated to optimize signal to noise ratio. Secondary antibodies used were Invitrogen's Alexa Fluor 488 donkey anti-goat IgG and Alexa 594 donkey anti-rabbit IgG in 3% BSA/0.1% TX-100/PBS (see **Table 4**). Each section was counterstained by using a premixed solution of 4, 6-diamidino-2-phenylindole (DAPI) (10μg/ml). After staining with secondary antibodies, the slides were washed with PBS and mounted with coverslips using AquaPolyMount. Images were collected using a fluorescence microscope using either a 10× or 20× objective. Analysis of Intratumor microvascular area (IMA) was conducted with MetaMorph^{TM} (Molecular Devices) software as described below.

2.4 Immunohistochemistry

Formalin-fixed paraffin-embedded sections (thickness 5 μm) underwent deparaffinization and antigen retrieval as in the immunofluorescence protocol. Endogenous peroxidases were then blocked by submerging the slides in 2.5% hydrogen peroxide/methanol buffer for 15 minutes. Nonspecific background was minimized using 0.3% bovine serum albumin in 0.1 mol/L Tris-buffered saline for 1 hour. Primary antibodies used were as described in **Table 5** and sections with primary antibodies were incubated 16-24 h at 4°C in humidity box. Secondary antibodies described in **Table 6** were applied for 30 minutes at room temperature.

The sections were then processed with an avidin-biotin-peroxidase complex (ImmPRESS; Vector Laboratories, Burlingame, CA), revealed in the presence of 3,3'-diaminobenzidine tetra hydrochloride (DAB; Sigma, St louis, MO).

Table 5: Primary antibodies used for Immunohistochemistry

Primary antibody	**Product**	**Species**	**dilution**
Anti-ThrRS	GTX116359	Rabbit	1:200
Anti-CD31	Biocare CP215A	Rabbit	1:100
Anti-F4/80	SC-25830	Mouse	1:100
Anti-SMactin	Sigma 1A4	Mouse	1:500
Anti-PECAM-1	SC-1506	Goat	1:100

Table 6: Secondary antibodies used for Immunohistochemistry

Secondary antibody	**spec**
Anti-rabbit IgG	DAKO Polymer-HRP goat
Anti-goat IgG	Jackson-HRP donkey

2.5 Intratumor quantification of MVD

MetaMorph offline software was used for computerized quantification of immunostained vascular structures (Chantrain, DeClerck et al. 2003). PECAM-1-postive pixels were selectively detected and uniformly displayed with green pixel overlay using the threshold function. With the command <Threshold Image> from the <Measure> menu, regions with heavily PECAM-1 staining were added, regions of counter-staining and background without PECAM-1 were deleted respectively and successively. These two steps were repeated until all the PECAM-1-positive pixels were selectively threshold. The threshold area corresponding to the PECAM-1 represented the intratumor microvascular area (IMA) and was measured with the <Region Measurement> function. For the whole section images, the PECAM-1(IMA) was selectively measured on the tumor tissue delineated by using the <Trace Region> command of MetaMorph. Neighboring connective tissue and necrotic areas were excluded from the selection. Similar procedures were done to TARS staining area (tumor area), the MVD was expressed as a ratio of PECAM-1-positive thresholded pixels to TARS positive staining area.

2.6 Statistical Analysis

All experiments were repeated at least 3 times with specific n-values reported within the Figure Legends. Data are presented as mean ± SEM, and $P < 0.05$ was considered significant. Pairwise comparisons were assessed using the Student's t-test.

CHAPTER 3: RESULTS

3.1 Mouse Model of Ovarian Cancer

To assess the relationship between TARS activity and ovarian cancer angiogenesis, a mouse model of ovarian cancer was established, a regimen of TARS inhibitor vs. vehicle was administered, and the microvessel density (MVD) of resulting ovarian tumors was detected by immunostaining and quantified by MetaMorph offline software. Comparisons were made to test the hypothesis that TARS activity promotes progression and angiogenesis of ovarian cancer.

Normal female C57BL/6 mice were used for assessment of the tumor formation. ID8-C3 cells were injected intraperitoneally (3×10^6 cells in 0.2 ml PBS). Animals were evaluated weekly for tumor growth and/or ascites accumulation. Intraperitoneal tumor formation was monitored by the accumulation of ascites fluid. Animals were euthanized approximately 10-24 days after the development of visible ascites, detected by abdominal swelling (**Fig. 2**). Immediately after euthanization, ascites fluid was collected from the peritoneal cavity. The peritoneal and thoracic cavities were opened. Solid tumors of varying size developed in the abdomen of mice by 5-6 weeks post-injection. The overall tumor take-rate was 100%. Tumor location and sizes were noted and amount of tumor on 11 tissues and organs was scored on a 0, +, ++, +++ scale: 0, no tumor evident by gross examination; +, tumors grossly evident on one organ or tissue, ++, moderate tumor formation on more than one organ or tissue; +++, extensive tumor formation on several organs or tissues (**Table 2 and Fig. 3**).

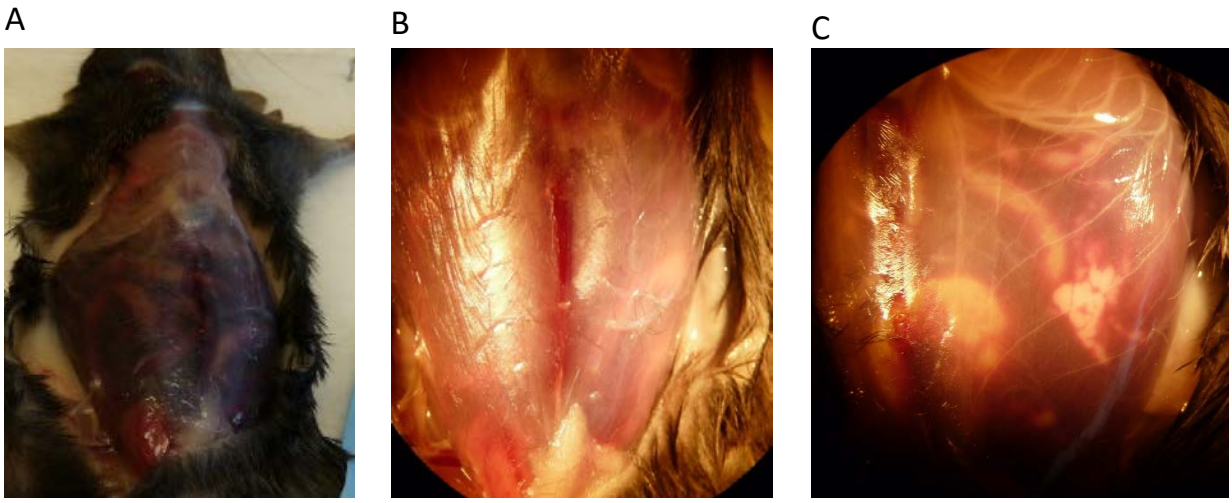

Figure 2. Development of ascites in syngeneic, orthotopic ID8-3 tumor model. C57BL/6 mice were injected with 3×10^6 ID8-3 ovarian cancer cells. Shown is the development of visible swelling due to the accumulation of ascites fluid 5 weeks after injection.

A. Mouse Anatomy

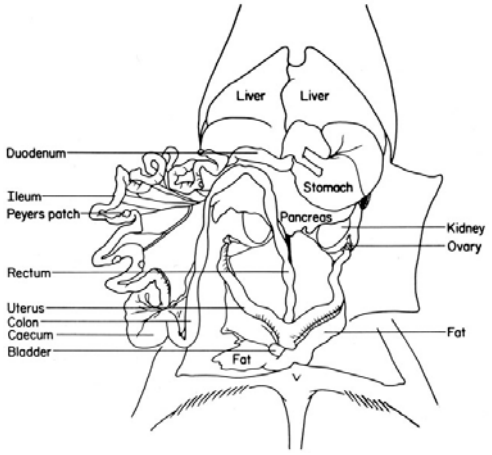

B. Abdominal Wall tumors

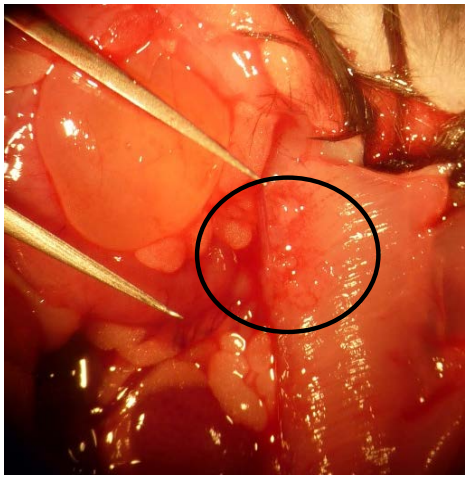

C. Stomach tumors

D. Mesenteric tumors

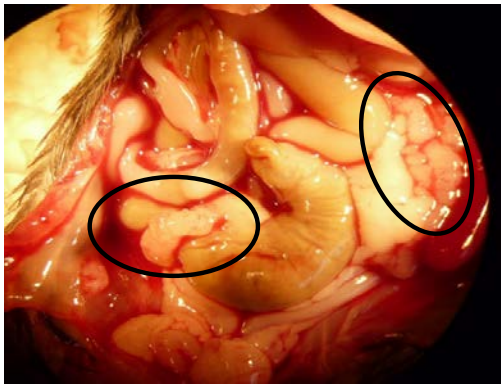

Figure 3. Generation of epithelial ovarian cancer in a syngeneic, orthotopic model. (A) Drawing of mouse anatomy ; (B,C,D) Gross anatomical pathology of representative mice, 5 weeks after ID8-3 intraperitoneal injection (B) Abdominal wall tumors, (C) Stomach tumors, and (D) Mesenteric tumors. These animals scored +++ on the tumor scale (**Table 2**).

3.1.1 ID8-C3 tumors express TARS and are angiogenic

Previous data from the Lounsbury lab demonstrated an increase in TARS staining in human ovarian cancer patient samples that correlated with progression of disease (Wellman, Eckenstein et al. 2014). To determine if the ID8-C3 model of ovarian cancer also overexpressed TARS, paraffin-embedded tumor samples were sectioned and stained to detect TARS using immunohistochemistry. As shown in **Fig. 4**, the ID8-C3 tumors exhibited heavy staining for TARS, suggesting that these tumors also overexpress TARS, thus serving as a good model for studying the role of TARS and tumor

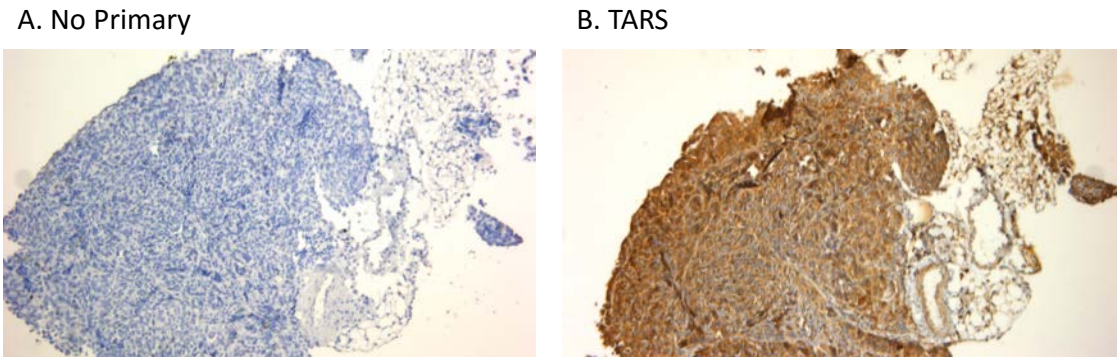

Figure 4. ID8-C3 ovarian tumors express high levels of TARS. Tumors were dissected from mice and then fixed, embedded, and sectioned. Sections were incubated with either normal mouse IgG (No Primary) or anti-TARS antibody and visualized by immunohistochemistry as described in the Methods.

angiogenesis.

Ovarian tumors in humans are known to induce angiogenesis, and anti-angiogenic therapy is offered to patients that have been resistant to standard therapies

(see Chapter 1). To show the angiogenic nature of the ID8-C3 ovarian cancer model, the angiogenic marker, α-smooth muscle actin (α-SMA), was detected in tumors by immunohistochemistry. The tumors exhibited angiogenesis (**Fig. 5**), however it was difficult to quantify the microvessel density using this technique, thus assessment of angiogenesis and quantification in later experiments was performed using

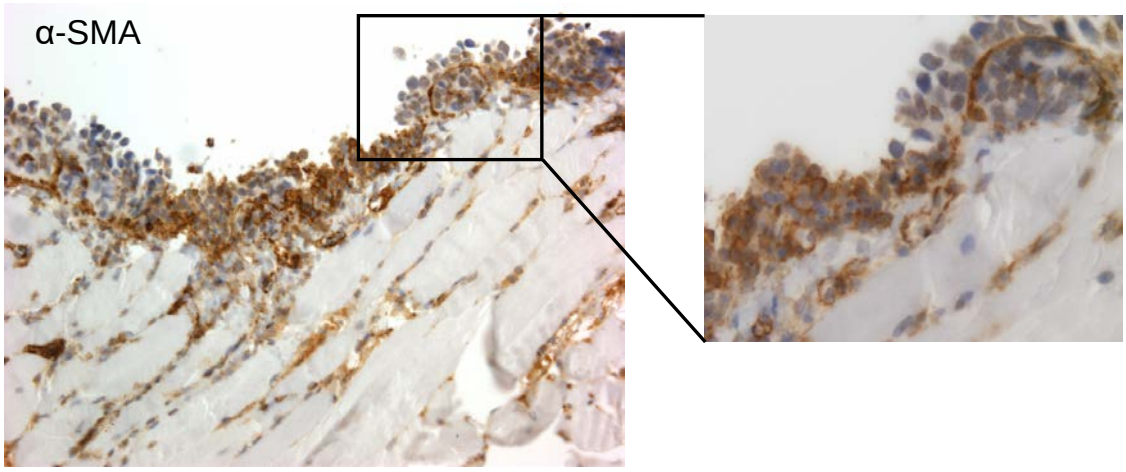

Figure 5. ID8-C3 tumors are angiogenic. Tumors attached to the abdominal wall were fixed and stained by immunohistochemistry to detect the blood vessel marker, α-smooth muscle actin (α-SMA). The inset shows a magnified section of the maturing blood vessel within the tumor tissue with attached abdominal muscle tissue.

immunofluorescence.

3.1.2 Summary of Ovarian Cancer Progression in the ID-8 Model

Mice receiving ID8-C3 cell injection into the abdomen displayed abdominal distension at approximately 4-5 weeks post-injection (**Fig. 2**). This abdominal distension was a result of the hemorrhagic ascites formation that was accompanied by peritoneal carcinomatosis. Tumor lesions were located throughout the peritoneum and were

observed on all visceral and peritoneal surfaces (**Fig. 3**). Gross and histological examination of the thoracic cavity did not show any metastasis to the lungs or liver, however one animal had a visible tumor on the kidney. Tumors displayed both a high level of TARS expression and were angiogenic (**Figs. 4,5**), suggesting that this model is appropriate for studying the effects of TARS inhibition on tumor progression and angiogenesis.

3.2 TARS inhibition with BC194 inhibits tumor progression

To determine a role for TARS in the progression of the ID8-C3 ovarian cancer model, mice were injected with ID8-C3 cells as in the baseline modeling, and after 3 weeks of tumor establishment, animals were weighed and injected with either vehicle or the TARS inhibitor BC194, three times per week for 3 weeks. There are 6 mice each for control and treatment group. The animal weights did not significantly differ between groups, however there was a significant reduction in the tumor progression score for the animals treated with BC194 (**Fig. 6**).

To compare the status of attaching and invading peritoneal organ sites, we examined tumor metastases on omentum, diaphragm, PW, liver, kidney, intestine and adipose tissue under a dissecting microscope (**Fig. 7**). We found that the omentum was the favored tissue for invasion of ID8 cells. The attachment and/or invasion of tumor cells to omentum were not significantly different between control and treatment mice, suggesting that BC194 did not affect cell adhesion and/or invasion ability at an early stage.

A

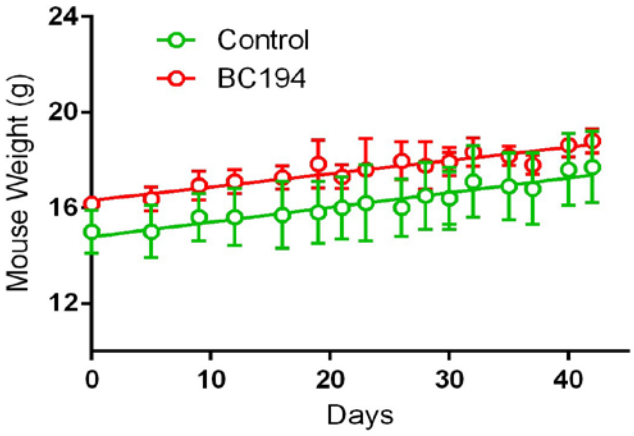

	Slope	Y-intercept
Control	0.06166 ± 0.004807	14.78 ± 0.1281
BC194	0.05538 ± 0.004785	16.32 ± 0.1275
p-value	0.36	<0.01

B

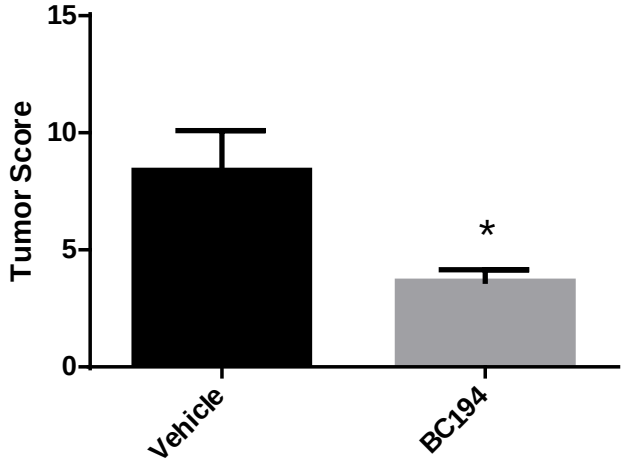

Figure 6. ID8-C3 Tumor Score is reduced by BC194 treatment. (A) The growth rate (slope) of animal weights is not different between the two groups. The curves were compared by linear regression analysis and there were 3 mice per group. (B) Tumor location and sizes were noted and amount of tumor on 11 tissues and organs was scored on a 0, +, ++, +++ scale: 0, no tumor evident by gross examination; +, tumors grossly evident on one organ or tissue; ++, moderate tumor formation on more than one organ or tissue; +++, extensive tumor formation on several organs or tissues. Significant difference of tumor progression score was observed between control and BC194 treatment groups. Data was analyzed with student's t-test, and n=6, p=0.017.

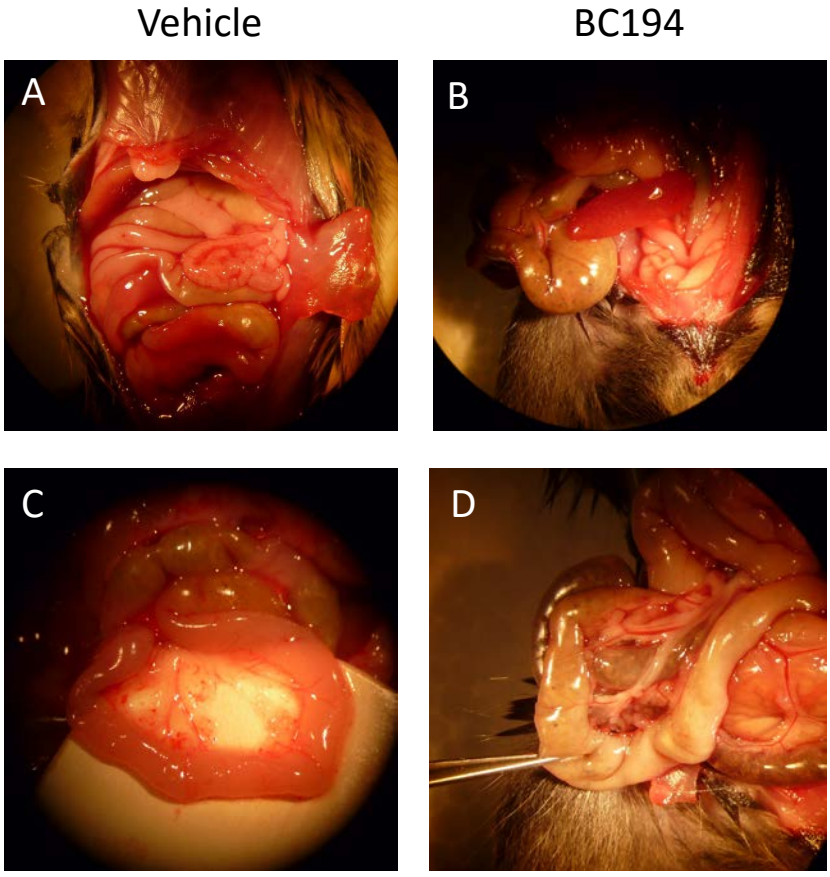

Figure 7. Inhibition of TARS with BC194 reduces the tumor burden of ID8-C3 ovarian cancer. Shown are representative images of mice after 6 weeks of tumor cell growth with injections of vehicle or BC194 beginning at 3 weeks. (A, B) represent abdominal cavity; (C, D) illustrate omental invasion.

3.3 Inhibition of TARS with BC194 inhibits angiogenesis

Immunofluorescent staining for the endothelial marker CD31 revealed distributed microvessels in the ID8 tumors with different degrees of vascular branching and irregularities. We examined whether the microvessel density could be quantified with the whole section scanning method. Using MetaMorph, we calculated the MVD on images of an entire ovarian tumor section generated by slide scanning and on a montage of serial microscopic field pictures. MetaMorph offline software was used for computerized quantification of immunostained vascular structures. PECAM-1 and TARS positive pixels were selectively detected and MVD was expressed as a ratio of PECAM-positive thresholded pixels to TARS.

In tumor sections with immunofluorescent staining, blood vessels and immune cells were observed. **Fig 8A** shows the endothelial vessel cells stained by CD31 (green), **Fig 8B** shows the combination of the blood vessel (green) and CD3+ T-cells (red), **Fig 8C** is a merged image of the tumor blood vessel (green) and nuclei (blue). The staining of endothelial cells was intensive, specific and easy to visualize for CD31. Tumors were frequently heterogeneous in their microvessel density, but the areas of highest neovascularization were found by scanning the tumor sections at low power (i.e., 10×objective lens and 10×ocular lens).

With the Metamorph system, we are able to generate the CD31 microvessel area (MVA) in tumor section images. Shown in **Fig 9 A** is the tumor mask created by TARS immunofluorescence and **Fig 9B** is the Metamorph image of CD31 staining. With the tumor mask and CD31 staining images, we are able to measure the microvessel density

(CD31 area/area of entire tissue spot). The MVD values were compared between BC194 treatment group and control group. The MVD (represented by tumor mask area) ranged from 0.181 to 0.469 in control, and from 0.008 to 0.128 in the BC194 treated. The treatment of BC194 reduced the MVD from an average of 0.331 to 0.106 and this difference was significant ($p<0.005$) (**Table 7**). These data together suggest that the effect of BC194 on the inhibition of tumor angiogenesis is related to the attenuation of ovarian tumor progression in this model of ovarian cancer.

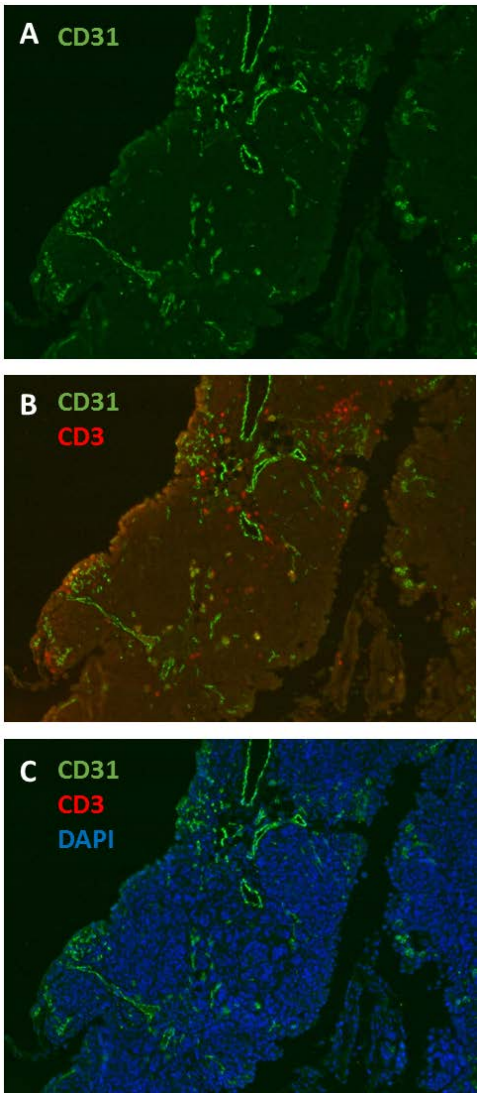

Figure 8. Representative staining of the blood vessel and immune cell markers in tumor sections. Immunofluorescent staining of mouse ovarian cancer tissues. The images shown are ×40 magnification immunofluorescence images of tissue tumor staining. (A) Endothelial vessel cells obtained from the CD31 staining (green) (B), Combined image of the tumor blood vessel (green) and CD3+ T-cells (red) (C) Combined image of the tumor blood vessel (green) and nuclei (blue).

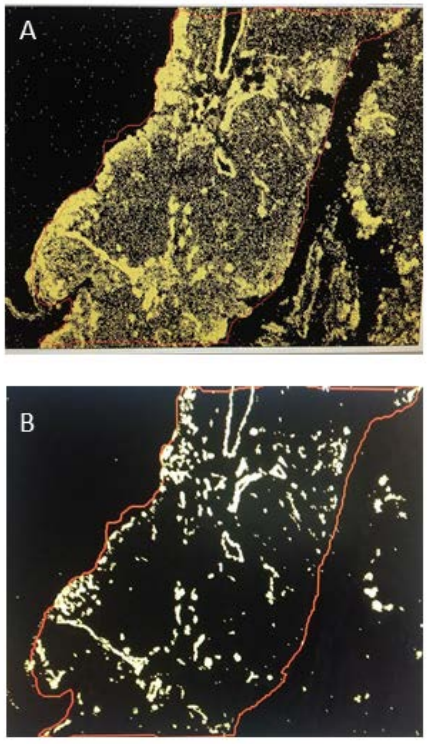

Figure 9. Representative tumor section showing the mask to generate the CD31 microvessel area (MVA) in Metamorph. **A,** TARS immunofluorescence from which the Metamorph algorithms create a tumor mask. **B,** The Metamorph image of CD31 staining generated by the mask. Microvessel density was defined as CD31 compartment area normalized to the tissue spot area (CD31 area/area of entire tissue).

Table 7. Relationship between BC194 treatment and microvessel density (MVD) determined by an anti-CD31 monoclonal antibody (CD31-TMA) in mouse ovarian tumors (n=7 for each group; $p<0.005$ by Student's *t*-test).

	CD31-MVD Vehicle	CD31-MVD BC194	*p*
	0.181893 0.469343 0.340097 0.345264 0.318466 0.366997 0.348977	0.107650 0.102280 0.105509 0.128095 0.086419 0.111219 0.148652	
Average (n=7)	**0.331**	**0.106**	**0.0026**
SEM	**0.0914**	**0.0133**	

CHAPTER 4: DISCUSSION AND FUTURE DIRECTIONS

Angiogenesis is critical for tumor growth. It was shown by many research groups that tumor neovascularity is associated with poor patient survival in a series of cancers. An increased MVD is positively correlated with early progression in a number of tumors. Such an association is likely due to increased supply of oxygen and nutrients by increased neovascularization in tumors. A high MVD is also more frequently observed in more actively proliferating tumors. Higher tumor vascularization also leads to an increased possibility for malignant cell infiltration and metastatic dissemination.

Several methods have been developed to measure the degree of angiogenesis, including determination of MVA, MVD. To date, MVD has been most extensively used to evaluate prognosis for various tumor types, but the results is inconsistent. The prognostic role of MVD is still unclear in ovarian cancer, one of the most vascular solid tumors. It was reported that increased MVD was associate with increasing nuclear grade, proliferative activity and frequency of metastasis, and higher microvessel count was observed in patients with metastasis than those disease free patients. In contrast, patients with a high MVD tumors were found to have a high 5-year survival rate. The existent of large-diameter may help to explain these conflicting findings, because large-diameter vascular channel lowers MVD and offsets the significance of MVD in evaluating the aggressiveness of the tumors.

Various models have been developed to study ovarian epithelial surface cells. In rodent models, human cancer cell have been used as xenografts in immunodeficient mice. One notable problem of these models is that there is no tumor and stromal cells

interactions because the immune system of the models are absent. It is especially concerned in ovarian cancer model because ovarian cancer is a disease where immune response is deeply involved in the carcinogenesis, progression and metastasis.

In this study we investigated the role of TARS in angiogenesis of ovarian tumors using a mouse model of ovarian cancer first described by Roby et al. The ID8 model was developed by propagating normal mouse ovarian epithelial cells until they developed a transformed phenotype. Transplantation of the cells by IP injection into standard C57BL/6 mice results in tumors and peritoneal ascites. As opposed to a xenograft model using human tumor lines in immunocompromised mice, the syngeneic nature of the ovarian models allows the tumor-stromal interaction characteristic of genuine cancers to be more accurately reproduced.

Previous data from the Lounsbury lab demonstrated an increase in TARS staining in human ovarian cancer patient samples that correlated with progression of disease (Wellman, Eckenstein et al. 2014). In order to assess the relationship between TARS activity and ovarian cancer angiogenesis and progression, we used the ID8 model and the borrelidin analog BC194 to specifically inhibit TARS. In this study, we observed that ID8 tumors exhibit heavy staining for TARS, suggesting the overexpression of TARS in tumors, thus serving as a good model for studying the role of TARS and tumor angiogenesis. Despite the widely used microvessel number counting from immunohistochemical staining (Hasan, Byers et al. 2002) , we observed that it was difficult to quantify the microvessel density of the ID8 tumors using this technique, so we

chose to use the immunofluorescence method to assess and quantify the microvessel density in experiments.

To determine whether inhibiting excess TARS function could reduce tumor progression, we treated mice with BC194, a TARS inhibitor. It was observed that in animals treated with BC194, the tumor progression score was significantly reduced suggesting that blocking TARS reduces ovarian tumor progression. Notably, the BC194 treatment did not result in any observed pathology or change in animal behavior. To assess whether the drop in tumor progression was related to TARS function in angiogenesis, we measured microvascular density in the tumors using CD31 immunofluorescence and computer image analysis. The data revealed that BC194 significantly reduces the MVD. All the above findings suggest that TARS may have a role in the angiogenesis in mouse ovarian cancer, and we propose that the reduced angiogenesis prevents the progression of ovarian cancer.

Although we successfully established the mouse model for the assessment of role of TARS, and developed the Metamorph system method to evaluate the microvessel density rather than manually counting the number of blood vessel, there are still some limitations in this study. First, more subject numbers are needed in order to achieve more rigorous data. Secondly, the staining methods for TARS and microvessels also need improvements. Third, the use of TARS as a possible diagnostic measure was not evaluated. These weaknesses can all be addressed in the future experiments.

Assessment of microvessel density is mostly done by manual counting of vascular profiles in tissue sections in which blood vessels are stained using antibodies

directed against endothelial cells (Weidner 1995). The most widely used protocol was described by Weidner et al., in which vessels are counted in the so-called 'angiogenic hot spot' (Weidner 1995). The hot spot is defined as the area of a tumor with the highest degree of vascularization. The hot spot is performed at low magnification and microvessel density measurements are performed at higher magnification. The outcome of the measurements is expressed either as the number of microvessels in hot spot or as the mean microvessel density assessed over a small number of highly vascularized areas of the tumor (van der Laak, Westphal et al. 1998). The selection of the hot spot is most critical in this protocol, because it has been shown to be subject to observer variation. The inter-observer variation limits the use of the hot spot procedure to construct reliable criteria for the prognostics of the metastasis of tumor. The objective selection criteria for both the hot spot and the microvessels are critically needed in order to achieve a reliable and reproducible hot-spot method.

Quantification of stained vessels can be achieved by measuring highest microvascular density (h-MVD), the average microvessel density (a-MVD) or the microvascular volume (MVV). Under low magnification (100× magnification), the area of highest microvascular density (the vascular hot spot) is located by scanning the section. In practice, three different areas are counted in order to localize the highest density. Three different fields are counted in each of these areas at 200× magnification, and the highest value taken as the h-MVD, expressed as vessels per mm^2. The measurement method for a-MVD is same as for h-MVD, and the mean of the vascular

counts obtained in at least 10-15 random fields is calculated for each tissue section. Results for a-MVD are expressed as mean ± standard deviation (vessels per mm^2).

The MVV is estimated by point counting using an eyepiece grid, which contains 100 points. Vessels that coincide with the points are counted in 15 fields selected randomly across each section (a total of 1500 points) and yields results expressed as percentage volume. Manual counting of microvessels is very subjective and may lead to huge interobserver variability, which may explain conflicting results (Vermeulen, Gasparini et al. 2002). A research was done to assess the efficacy and consistence between manually counting the number of microvessels in a subjectively selected hot spot and the interactive and automated image processing methods in the same complete tumor sections.

The Chalkley method is similar to that used to determine the MVV. First, the areas that appear to have the maximum number of discrete microvessels is identified at low magnification. An eyepiece grid containing 25 randomly positioned dots is rotated at higher magnifications to make the maximum numbers of points are on or within the vessels of the vascular hot spot. Instead of counting the individual microvessels, the overlying dots are counted. In cohort of patients with breast carcinoma, a significant correlation was found between MVD assessment by the Weidner method and Chalkley point counting. A significant reduction in OS was observed between patients stratified by Chalkley count in both univariate and multivariate analysis. The Chalkley score was also found the most significant independent predictor of outcome in

another study in patients with node-positive breast carcinoma (Vermeulen, Gasparini et al. 2002).

The first problem arising with these quantification methods is the selection of a representative tumor block. In one research, MVD in in-situ growth regions is found approximately half of that seen in invasive regions in colorectal adenocarcinoma, suggesting that multiple blocks should be assessed. The de Jong et al group found that when more than one tissue block was analyzed compared to only counts within sections of one block were examined, a higher average coefficient of variation was achieved, indicating that a comprehensive inspection of available tumor material is needed to identify the relevant hot spots.

Another factor that influences the identification of the vascular hot spot is the training and experience of the investigator. In a research done by Barbareschi et al, MVD in 91 node negative invasive breast carcinomas measured by two pathologist of different experience was compared, only the counts of the experienced pathologist were significantly associated with relapse-free survival (Bevilacqua, Barbareschi et al. 1995). Similar results were noted in another series of node negative breast cancer patients. Once the vascular hot spot is identified, vessel counting appears to be less variable than the process of hot spot selection.

There is an automated counting technique (CIAS) that improves reproducibility and reduces inter-observer variability and has been proposed as a more objective method of assessing MVD (Charpin, Garcia et al. 1997). In a series of 91 node-negative invasive ductal carcinomas of the breast, both the number of CD31 positive microvessels

measured by an experienced observer and the microvessel area (MVA) determined by CIAS were independently associated with recurrence-free survival (Charpin, Garcia et al. 1997). The main advantage of CIAS is the additional morphometric parameters that can be detected the number of vessels with a certain dimension range, the vessel luminal area, vessel luminal perimeter and the number of immunostained areas per microscopic field. MVD can be measured more objectively without the intervention of an investigator. The apparent disadvantage of CIAS is the time consuming nature of the method and its higher cost. These systems are not fully automated yet and require a high degree of operator interaction. The vascular hot spot is still identified manually before automated counting as the heterogeneity of microvessel morphology and immunostaining intensity particularly hampers a fully automated analysis of tumor MVD.

Taking these studies into consideration, our angiogenesis quantification method had strengths with respect to its computer analysis rather than counting vessels by eye, however using more samples and developing a CIAS-like method for unbiased selection of area for quantification would improve the reliability of results. Future directions would also include a study of overexpressed TARS in the implanted ID8 cells where we would expect the resulting tumors have enhanced angiogenesis. A current analysis is being done in the Lounsbury lab of subcutaneous ID-8 tumors which will be a better model to quantify primary tumor size.

Another important parameter that remains to be studied is the use of TARS levels as a diagnostic in ovarian cancer. We found that TARS is overexpressed in the ID8 tumors, and we collected serum and ascites fluid from the animals used in this study. An

important future study would be to measure TARS levels in these samples to correlate the progression of disease with levels of TARS. We predict that TARS in serum and especially ascites fluid will be elevated as the ovarian tumors progress. Together these studies suggest an important role for TARS in the angiogenesis and progression of ovarian cancer, and TARS should be pursued as a possible future therapeutic target in human ovarian cancer.

COMPREHENSIVE BIBLIOGRAPHY

Abulafia, O., W. E. Triest and D. M. Sherer (1997). "Angiogenesis in primary and metastatic epithelial ovarian carcinoma." Am J Obstet Gynecol **177**(3): 541-547.

Baba, T., M. Mandai and S. Fujii (2004). "[Peritoneal dissemination of ovarian cancer and tumor angiogenesis]." Nihon Rinsho **62 Suppl 10**: 467-470.

Bamberger, E. S. and C. W. Perrett (2002). "Angiogenesis in epithelian ovarian cancer." Mol Pathol **55**(6): 348-359.

Bevilacqua, P., M. Barbareschi, P. Verderio, P. Boracchi, O. Caffo, P. Dalla Palma, S. Meli, N. Weidner and G. Gasparini (1995). "Prognostic value of intratumoral microvessel density, a measure of tumor angiogenesis, in node-negative breast carcinoma--results of a multiparametric study." Breast Cancer Res Treat **36**(2): 205-217.

Brooks, P. C., R. A. Clark and D. A. Cheresh (1994). "Requirement of vascular integrin alpha v beta 3 for angiogenesis." Science **264**(5158): 569-571.

Brown, M. R., J. O. Blanchette and E. C. Kohn (2000). "Angiogenesis in ovarian cancer." Baillieres Best Pract Res Clin Obstet Gynaecol **14**(6): 901-918.

Cancer Genome Atlas Research, N. (2011). "Integrated genomic analyses of ovarian carcinoma." Nature **474**(7353): 609-615.

Chantrain, C. F., Y. A. DeClerck, S. Groshen and G. McNamara (2003). "Computerized quantification of tissue vascularization using high-resolution slide scanning of whole tumor sections." J Histochem Cytochem **51**(2): 151-158.

Charpin, C., S. Garcia, C. Bouvier, F. Martini, L. Andrac, P. Bonnier, M. N. Lavaut and C. Allasia (1997). "CD31/PECAM automated and quantitative immunocytochemical assays in breast carcinomas: correlation with patient follow-up." Am J Clin Pathol **107**(5): 534-541.

Christie, M. and M. K. Oehler (2006). "Molecular pathology of epithelial ovarian cancer." J Br Menopause Soc **12**(2): 57-63.

Darai, E., A. F. Bringuier, F. Walker-Combrouze, A. Fauconnier, A. Couvelard, G. Feldmann, P. Madelenat and J. Y. Scoazec (1998). "CD31 expression in benign, borderline, and malignant epithelial ovarian tumors: an immunohistochemical and serological analysis." Gynecol Oncol **71**(1): 122-127.

Eliceiri, B. P., R. Klemke, S. Stromblad and D. A. Cheresh (1998). "Integrin alphavbeta3 requirement for sustained mitogen-activated protein kinase activity during angiogenesis." J Cell Biol **140**(5): 1255-1263.

Erickson, B. K., M. G. Conner and C. N. Landen, Jr. (2013). "The role of the fallopian tube in the origin of ovarian cancer." Am J Obstet Gynecol **209**(5): 409-414.

Glass, K., J. Quackenbush, D. Spentzos, B. Haibe-Kains and G. C. Yuan (2015). "A network model for angiogenesis in ovarian cancer." BMC Bioinformatics **16**: 115.

Greenaway, J., R. Moorehead, P. Shaw and J. Petrik (2008). "Epithelial-stromal interaction increases cell proliferation, survival and tumorigenicity in a mouse model of human epithelial ovarian cancer." Gynecol Oncol **108**(2): 385-394.

Greenblatt, M. S., W. P. Bennett, M. Hollstein and C. C. Harris (1994). "Mutations in the p53 tumor suppressor gene: clues to cancer etiology and molecular pathogenesis." Cancer Res **54**(18): 4855-4878.

Habibi, D., N. Ogloff, R. B. Jalili, A. Yost, A. P. Weng, A. Ghahary and C. J. Ong (2012). "Borrelidin, a small molecule nitrile-containing macrolide inhibitor of threonyl-tRNA synthetase, is a potent inducer of apoptosis in acute lymphoblastic leukemia." Invest New Drugs **30**(4): 1361-1370.

Hasan, J., R. Byers and G. C. Jayson (2002). "Intra-tumoural microvessel density in human solid tumours." Br J Cancer **86**(10): 1566-1577.

Hassan, R., A. T. Remaley, M. L. Sampson, J. Zhang, D. D. Cox, J. Pingpank, R. Alexander, M. Willingham, I. Pastan and M. Onda (2006). "Detection and quantitation of serum mesothelin, a tumor marker for patients with mesothelioma and ovarian cancer." Clin Cancer Res **12**(2): 447-453.

He, L., Q. Wang and X. Zhao (2015). "Microvessel density as a prognostic factor in ovarian cancer: a systematic review and meta-analysis." Asian Pac J Cancer Prev **16**(3): 869-874.

Hollingsworth, H. C., E. C. Kohn, S. M. Steinberg, M. L. Rothenberg and M. J. Merino (1995). "Tumor angiogenesis in advanced stage ovarian carcinoma." Am J Pathol **147**(1): 33-41.

Howard, O. M., H. F. Dong, D. Yang, N. Raben, K. Nagaraju, A. Rosen, L. Casciola-Rosen, M. Hartlein, M. Kron, D. Yang, K. Yiadom, S. Dwivedi, P. H. Plotz and J. J. Oppenheim (2002). "Histidyl-tRNA synthetase and asparaginyl-tRNA synthetase, autoantigens in myositis, activate chemokine receptors on T lymphocytes and immature dendritic cells." J Exp Med **196**(6): 781-791.

Jordanova, A., J. Irobi, F. P. Thomas, P. Van Dijck, K. Meerschaert, M. Dewil, I. Dierick, A. Jacobs, E. De Vriendt, V. Guergueltcheva, C. V. Rao, I. Tournev, F. A. Gondim, M. D'Hooghe, V. Van Gerwen, P. Callaerts, L. Van Den Bosch, J. P. Timmermans, W. Robberecht, J. Gettemans, J. M. Thevelein, P. De Jonghe, I. Kremensky and V. Timmerman (2006). "Disrupted function and axonal distribution of mutant tyrosyl-tRNA synthetase in dominant intermediate Charcot-Marie-Tooth neuropathy." Nat Genet **38**(2): 197-202.

Kaku, T., S. Watanabe and Y. Ohishi (2012). "[Pathology of ovarian cancer]." Nihon Rinsho **70 Suppl 4**: 512-516.

Kelly, Z. L., A. Michael, S. Butler-Manuel, H. S. Pandha and R. G. Morgan (2011). "HOX genes in ovarian cancer." J Ovarian Res **4**: 16.

Liu, J., G. Yang, J. A. Thompson-Lanza, A. Glassman, K. Hayes, A. Patterson, R. T. Marquez, N. Auersperg, Y. Yu, W. C. Hahn, G. B. Mills and R. C. Bast, Jr. (2004). "A genetically defined model for human ovarian cancer." Cancer Res **64**(5): 1655-1663.

Marcinkiewicz, C., Y. Taooka, Y. Yokosaki, J. J. Calvete, M. M. Marcinkiewicz, R. R. Lobb, S. Niewiarowski and D. Sheppard (2000). "Inhibitory effects of MLDG-containing heterodimeric disintegrins reveal distinct structural requirements for interaction of the integrin alpha 9beta 1 with VCAM-1, tenascin-C, and osteopontin." J Biol Chem **275**(41): 31930-31937.

Massi, D., A. Franchi, L. Borgognoni, M. Paglierani, U. M. Reali and M. Santucci (2002). "Tumor angiogenesis as a prognostic factor in thick cutaneous malignant melanoma. A quantitative morphologic analysis." Virchows Arch **440**(1): 22-28.

Mirando, A. C., K. Abdi, P. Wo and K. M. Lounsbury (2016). "Assessing the effects of threonyl-tRNA synthetase on angiogenesis-related responses." Methods.

Moss, S. J., I. Carletti, C. Olano, R. M. Sheridan, M. Ward, V. Math, E. A. M. Nur, A. F. Brana, M. Q. Zhang, P. F. Leadlay, C. Mendez, J. A. Salas and B. Wilkinson (2006). "Biosynthesis of the angiogenesis inhibitor borrelidin: directed biosynthesis of novel analogues." Chem Commun (Camb)(22): 2341-2343.

Mutch, D. G. and J. Prat (2014). "2014 FIGO staging for ovarian, fallopian tube and peritoneal cancer." Gynecol Oncol **133**(3): 401-404.

Offersen, B. V., M. Borre, F. B. Sorensen and J. Overgaard (2002). "Comparison of methods of microvascular staining and quantification in prostate carcinoma: relevance to prognosis." APMIS **110**(2): 177-185.

Ordonez, N. G. (2007). "What are the current best immunohistochemical markers for the diagnosis of epithelioid mesothelioma? A review and update." Hum Pathol **38**(1): 1-16.

Orre, M., M. Lotfi-Miri, P. Mamers and P. A. Rogers (1998). "Increased microvessel density in mucinous compared with malignant serous and benign tumours of the ovary." Br J Cancer **77**(12): 2204-2209.

Paley, P. J. (2002). "Angiogenesis in ovarian cancer: molecular pathology and therapeutic strategies." Curr Oncol Rep **4**(2): 165-174.

Paley, P. J., B. A. Goff, A. M. Gown, B. E. Greer and E. H. Sage (2000). "Alterations in SPARC and VEGF immunoreactivity in epithelial ovarian cancer." Gynecol Oncol **78**(3 Pt 1): 336-341.

Perets, R., G. A. Wyant, K. W. Muto, J. G. Bijron, B. B. Poole, K. T. Chin, J. Y. Chen, A. W. Ohman, C. D. Stepule, S. Kwak, A. M. Karst, M. S. Hirsch, S. R. Setlur, C. P. Crum, D. M. Dinulescu and R. Drapkin (2013). "Transformation of the fallopian tube secretory epithelium leads to high-grade serous ovarian cancer in Brca;Tp53;Pten models." Cancer Cell **24**(6): 751-765.

Peterson, C. M., R. Reed, C. J. Jolles, K. P. Jones, R. C. Straight and A. M. Poulson (1992). "Photodynamic therapy of human ovarian epithelial carcinoma, OVCAR-3, heterotransplanted in the nude mouse." Am J Obstet Gynecol **167**(6): 1852-1855.

Plow, E. F., T. A. Haas, L. Zhang, J. Loftus and J. W. Smith (2000). "Ligand binding to integrins." J Biol Chem **275**(29): 21785-21788.

Roberts, P. C., E. P. Mottillo, A. C. Baxa, H. H. Heng, N. Doyon-Reale, L. Gregoire, W. D. Lancaster, R. Rabah and E. M. Schmelz (2005). "Sequential molecular and cellular events during neoplastic progression: a mouse syngeneic ovarian cancer model." Neoplasia **7**(10): 944-956.

Roby, K. F., C. C. Taylor, J. P. Sweetwood, Y. Cheng, J. L. Pace, O. Tawfik, D. L. Persons, P. G. Smith and P. F. Terranova (2000). "Development of a syngeneic mouse model for events related to ovarian cancer." Carcinogenesis **21**(4): 585-591.

Sherman-Baust, C. A., E. Kuhn, B. L. Valle, M. Shih Ie, R. J. Kurman, T. L. Wang, T. Amano, M. S. Ko, I. Miyoshi, Y. Araki, E. Lehrmann, Y. Zhang, K. G. Becker and P. J. Morin (2014). "A genetically engineered ovarian cancer mouse model based on fallopian tube transformation mimics human high-grade serous carcinoma development." J Pathol **233**(3): 228-237.

Taskin, S., Y. Gumus, S. Kiremitci, K. Kahraman, A. Sertcelik and F. Ortac (2012). "Malignant peritoneal mesothelioma presented as peritoneal adenocarcinoma or primary ovarian cancer: case series and review of the clinical and immunohistochemical features." Int J Clin Exp Pathol **5**(5): 472-478.

van der Laak, J. A., J. R. Westphal, L. J. Schalkwijk, M. M. Pahlplatz, D. J. Ruiter, R. M. de Waal and P. C. de Wilde (1998). "An improved procedure to quantify tumour vascularity using true colour image analysis. Comparison with the manual hot-spot procedure in a human melanoma xenograft model." J Pathol **184**(2): 136-143.

Vaughan, S., J. I. Coward, R. C. Bast, Jr., A. Berchuck, J. S. Berek, J. D. Brenton, G. Coukos, C. C. Crum, R. Drapkin, D. Etemadmoghadam, M. Friedlander, H. Gabra, S. B. Kaye, C. J. Lord, E. Lengyel, D. A. Levine, I. A. McNeish, U. Menon, G. B. Mills, K. P. Nephew, A. M. Oza, A. K. Sood, E. A. Stronach, H. Walczak, D. D. Bowtell and F. R. Balkwill (2011). "Rethinking ovarian cancer: recommendations for improving outcomes." Nat Rev Cancer **11**(10): 719-725.

Vermeulen, P. B., G. Gasparini, S. B. Fox, C. Colpaert, L. P. Marson, M. Gion, J. A. Belien, R. M. de Waal, E. Van Marck, E. Magnani, N. Weidner, A. L. Harris and L. Y. Dirix (2002). "Second international consensus on the methodology and criteria of evaluation of angiogenesis quantification in solid human tumours." Eur J Cancer **38**(12): 1564-1579.

Wakasugi, K. and P. Schimmel (1999). "Two distinct cytokines released from a human aminoacyl-tRNA synthetase." Science **284**(5411): 147-151.

Walton, J., J. Blagih, D. Ennis, E. Leung, S. Dowson, M. Farquharson, L. A. Tookman, C. Orange, D. Athineos, S. Mason, D. Stevenson, K. Blyth, D. Strathdee, F. R. Balkwill, K. Vousden, M. Lockley and I. A. McNeish (2016). "CRISPR/Cas9-Mediated Trp53 and Brca2 Knockout to Generate Improved Murine Models of Ovarian High-Grade Serous Carcinoma." Cancer Res **76**(20): 6118-6129.

Weidner, N. (1995). "Intratumor microvessel density as a prognostic factor in cancer." Am J Pathol **147**(1): 9-19.

Wellman, T. L., M. Eckenstein, C. Wong, M. Rincon, T. Ashikaga, S. L. Mount, C. S. Francklyn and K. M. Lounsbury (2014). "Threonyl-tRNA synthetase overexpression correlates with angiogenic markers and progression of human ovarian cancer." BMC Cancer **14**: 620.

Wild, R., S. Ramakrishnan, J. Sedgewick and A. W. Griffioen (2000). "Quantitative assessment of angiogenesis and tumor vessel architecture by computer-assisted digital image analysis: effects of VEGF-toxin conjugate on tumor microvessel density." Microvasc Res **59**(3): 368-376.

Williams, T. F., A. C. Mirando, B. Wilkinson, C. S. Francklyn and K. M. Lounsbury (2013). "Secreted Threonyl-tRNA synthetase stimulates endothelial cell migration and angiogenesis." Sci Rep **3**: 1317.

Wong, C., T. L. Wellman and K. M. Lounsbury (2003). "VEGF and HIF-1alpha expression are increased in advanced stages of epithelial ovarian cancer." Gynecol Oncol **91**(3): 513-517.